

Design and Simulation of Multi Stage Fly Back Photo Voltaic Conversion System

N.Manimaran

Assistant Professor

Department of EEE

Adhiparasakthi Engg. College

Melmaruvathur

Email:manimaran04@gmail.com

A. Prakasam

Assistant Professor

Department of EEE

Adhiparasakthi Engg. College

Melmaruvathur

Email:prakasam007@gmail.com

C. Kathiravan

Assistant Professor

Department of EEE

Adhiparasakthi Engg. College

Melmaruvathur

Email:kadhiravanc@gmail.com

J. Madhavan

Assistant Professor

Department of EEE

Adhiparasakthi Engg. College

Melmaruvathur

Email: madhavan.m.e@gmail.com

Abstract—An electrolytic capacitor used as a decoupling reservoir which restrict the lifetime of photovoltaic (PV) micro inverters. . The project focuses on selection of the minimum decoupling capacitor value for the proper operation of discontinuous conduction mode fly back PV micro inverter by considering the total harmonic distortion (THD) and PV power utilization ratio. A decoupling capacitor selection method for single-stage and two-stage fly back inverters is proposed. For two stage inverters, the control method of the dc-dc converter determines the stage where the decoupling function takes place. Thus, the PV side decoupling capacitor should be dimensioned according to the PV power utilization ratio, and the inverter side decoupling capacitor should be selected according to the desired THD limitation. The corresponding voltage ripple limits for THD and PV power utilization ratio satisfy the IEC standard values of 5% and 9.6%, respectively.

I. INTRODUCTION

The growing environmental concerns and non-renewable nature associated with the use of fossil fuels, such as oil, coal, natural gas, etc. Solar energy has proven to be a very attractive solution for the growing energy need in the world due to several advantages, such as its availability in abundance, pollution-free power generation, inexhaustible nature, etc[1]. The ac module is the integration of the PV panel and a small grid-tied inverter in one electrical device to harvest the energy[3,4]. The ac model performs maximum power point tracking (MPPT) of the PV panel, voltage amplification, galvanic isolation, and injection of high-quality ac to the utility grid.

The conversion of dc-ac power within the PV module can be done in single stage or multiple stages [19], [1]-[8] commonly used is two stage converter in this application [10], [21]-[26]. There are two stages of power conversion in this configuration. The first stage is the dc-dc conversion gives galvanic isolation and boost up the voltage. In the second stage which operates as inverter provides high quality current to the grid. However the two stage model is very easy to do and simple, it has some important demerits. Due to the presence of two stages of power conversion the efficiency is limited and density of the power is reduced by two stages. In addition the soft switching technique for the second stage of the converter is inconvenient. Here usually a low switching frequency pulse width modulation inverter is used to reduce the unavoidable switching losses in the switches. Low frequency operation increases the size and loss of filter to eliminate the high frequency signals and to provide quality current to the utility grid. The flyback topology is proposed for switches and lead to lossless and compact solution at the interface of PV panel and the grid.

The flyback concept proves to be reliable and cost effective topology which uses number of semiconductor switches in PV modules [11]. The switches operating under ZVS condition the switching losses due to hard switching is strongly reduced at high frequencies. The continuous conduction mode is not feasible in flyback inverter because the inverter acts as a load independent voltage source due to improper discharge of the magnetizing inductance in the transformer [17]. In accordance discontinuous conduction mode is very convenient for flyback inverters however, the current and voltage stress are more on the switches. By analysing the conventional flyback inverters hard switching technique results in low efficiency [11]. A soft switching technique is used in flyback inverters achieved by the actively switched snubber circuit parallel to the primary switch [1]. By increase in number of active and passive components, the system complexity also increases. In flyback inverters to achieve soft switching active clamps are used commonly and to clamp the voltage across the switch [18], [19]. But the switch in primary side is soft switched by active clamped and the switch used in clamp circuit is usually hard switched.

II. OPERATING PRINCIPLES OF THE PROPOSED SYSTEM

A. Review Stage

The limitations of the existing topologies can be overcome by using soft-switching techniques for the switches. To achieve soft switching primary switch additional circuits are required for flyback topologies. Besides the transfer of power is limited when flyback inverter operation in discontinuous conduction mode. For this reason, a new technique to achieve ZVS for the primary switch is done in this paper. The secondary switches are also soft switched by using the negative current

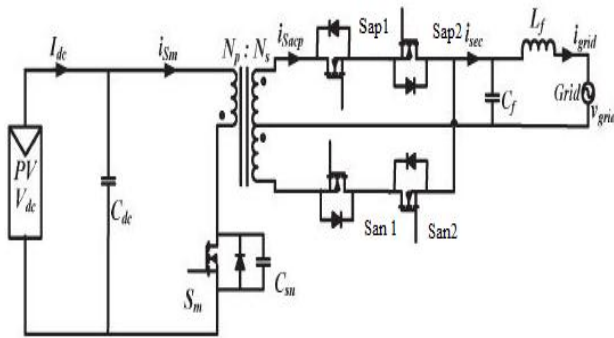


Fig 1. Proposed flyback inverter scheme.

The soft switching of the primary switch circuit diagram is shown in figure 1. The proposed topology consists of center tapped flyback transformer, an input decoupling capacitor, primary switches bidirectional switches on the secondary side and an output filter. The primary switch S_p is triggered to charge the magnetizing inductance to reference current. Based on the grid frequency and sinusoidal waveform the peak current varies. The energy stored in the transformer is injected to the grid by switching ON either S_{ap1} or S_{an1} during the positive or negative half cycle simultaneously. The secondary current moves to zero for each switching cycle, where the bidirectional switch is turned on allowing the current to reverse its direction. As a result, the magnetic inductance gets charged in the reverse direction. By comparing the negative peak of the inductor current with grid frequency results in control of charging.

MODE I: This mode starts by switching on primary side switch s_p . The secondary switches $S1$ & $S2$ are made on during the entire positive and negative cycle simultaneously. At this time the primary side magnetizing inductance L_m receives the voltage of the PV panel hence the current in the inductance get increased. The switch current is denoted by.

$$ISP(t) = \frac{v_{dc}}{l_m}(t) - I_{sp_PEAK} \quad (1)$$

The peak of the primary current $i_{sm_pk_p}$ is dependent on the instantaneous value of the ac output power as the amount of energy transfer to output is governed by the magnetizing inductor current. Further, the dc from the PV can be related to the inductor current by averaging inductor current over the switching cycle.

MODE II: The switch s_m is turned off at beginning of the interval, where as secondary switching remain ON. Due to the presence of output capacitor across the primary MOSFET, the drain-source voltage cannot increase instantly to a high voltage. The rise of the drain- source voltage across the switch s_m is slowed down because of charging of capacitor c_{sn} . The transition from the ON state to the OFF state of switch s_m occurs within a very short interval of time.

$$I_{avg} = \frac{L_m}{2V_{dc}T_s} (i_{sm_pk_p}^2 - i_{sm_pk_n}^2) \quad (2)$$

MODE III: Once the capacitor C_{sn} is completely charged to its maximum value, the energy stored in the magnetizing inductor of the transformer is transferred to the grid. This is made possible by either the secondary switch S_{ap1} or S_{an1} depending on the positive or negative half-cycle of the during the interval. Since the magnetizing inductance L_m was charged in the reverse direction in the previous interval, the inductor current flows in the direction to transfer the energy stored in L_m to the input capacitor. As a result, the primary current i_{sm} is negative during this interval. The voltage across switch S_m starts to decrease slowly as the capacitor across the switch starts to discharge. This mode comes to an end with the complete discharge of the capacitor across the switch

MODE IV: since the capacitor is completely discharged, the drain-source voltage of the primary switch S_m nearly equals zero. It causes the antiparallel diode of the switch to conduct. the primary switch can be turned on with ZVS during this interval.

The high frequency component present in the secondary current is filtered by the output filter such that the average value of the secondary current during the switching interval T_s is obtained by integrating over the period.

B. Figures

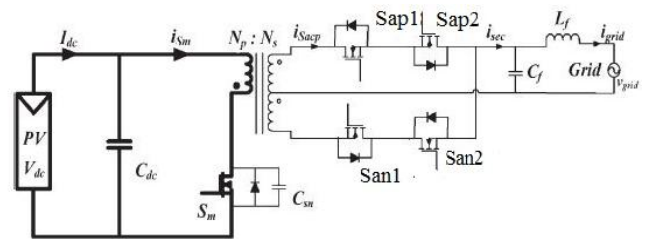


Fig 3 Mode 1

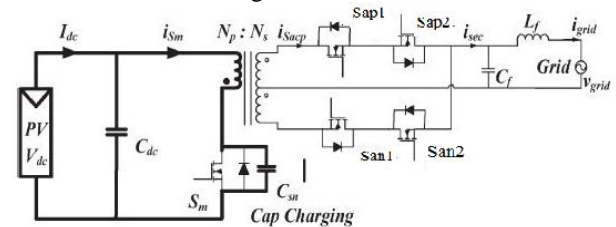


Fig 4 Mode 2

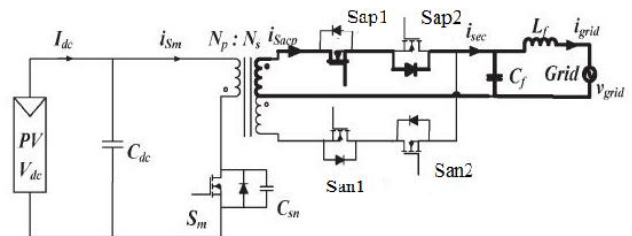


Fig 5 Mode 3

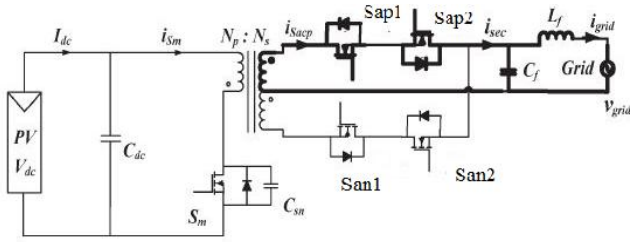


Fig 6 Mode 4

TABLE I
INVERTER PARAMETERS

Symbol	Quantity	value
Po	Output power	250w
Vdc	Input voltage	40-70V DC
Vgrid	Grid Voltage	230V AC
fsw	Switching Frequency	30KHz-65KHz
Cpv	Input capacitor	5mf
Flyback transformer		
Np: Ns	Turn's ratio	1:5
Lm	Magnetizing inductance	23μH
Np	No of turns in primary	11
Bmax	Peak magnetic flux density	0.23T
Ig	Air gap length	0.395cm
Lleakage	Leakage Inductance	1.75μH
	Core Type	EE55

$$d_2 + d_3 = (1 - d_1)(3)$$

$$(1 - d_1)Ts = \frac{(i_{sm_pk_p} + i_{sm_pk_n})NL_m}{V_{ac}} \quad (4)$$

$$Vac = Vac_pk \sin \omega t \quad (5)$$

$$iac = Iac_pk \sin \omega t \quad (6)$$

$$Ts(\omega t) = t_{ON}(\omega t) + t_{OFF}(\omega t) \quad (7)$$

$$t_{ON}(\omega t) = t_{ON_pk} \sin(\omega t) \quad (8)$$

III. DESIGN OF CONTROLLER AND LOSS ANALYSIS

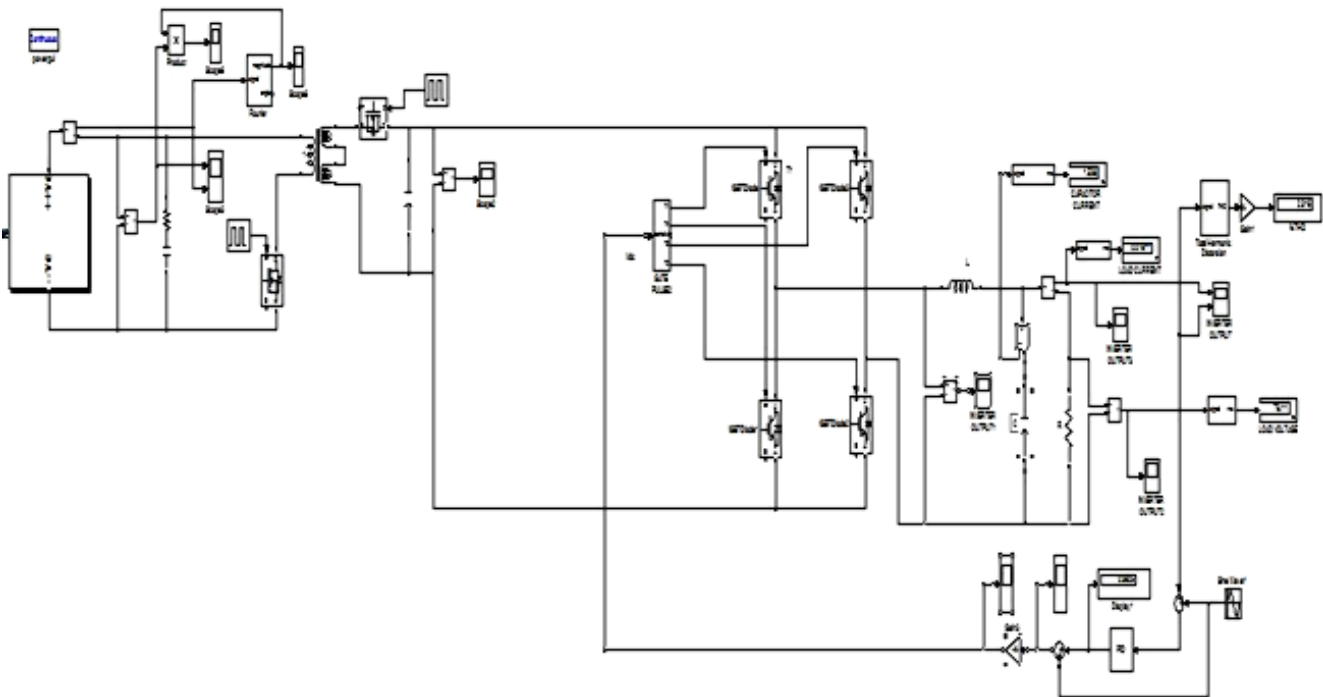
The model explains that a PI control technique is used to control the output grid current. The proportional and integral gain is calculated and designed according to the grid voltage to the inverter side triggering. The controller's proportional gain Kp is 0.027 and integral gain Ki is 1. The loss calculation is carried out for nominal operating condition for input power 300 Wat input dc voltage of 48 V.The MOSFETs of the proposed inverterovercomes many losses to improve the

efficiency isdone here. The primary side losses depends the rmscurrent through the primary switch.

$$P_{cond} = I_{sm_rms}^2 R_{ds_on} = 2.1W. \quad (9)$$

IV. RESULT OF PROPOSED SIMULATION

A 300-W flyback inverter was designed and simulated in physical security information management software with the component values obtained from the design procedure aforementioned are listed in Table 1.The switch current ism, drain source voltage, and the gating for the primary switch.The negative current shown in the figure is due to the reverse charging of magnetizing inductance of the transformer, the discharge of drain-source capacitance. A simple capacitive snubber is used to reduced the voltage spikes observed across the primary switch at turn OFF in the simulationThe



secondary side also soft-switched at turn ON. The variation of the primary switch voltage and the switch current over the cycle for an input dc voltage of 48V is shown. A pair of secondary MOSFETs switches at line frequency. The gating of the secondary MOSFETs along with the switch current for the positive half-cycle. Whereas the closed-loop output current and the grid voltage waveforms. The gating of the secondary side is provided by the grid side voltage and the inverter output with the control of PI control. The simulation results are given below.

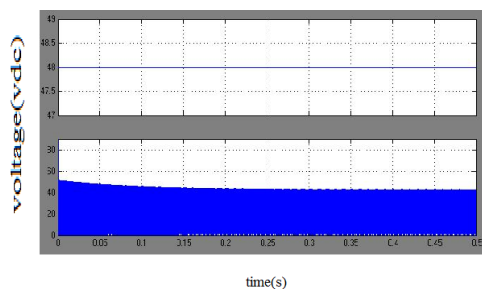


Fig 7. Solar panel input voltage

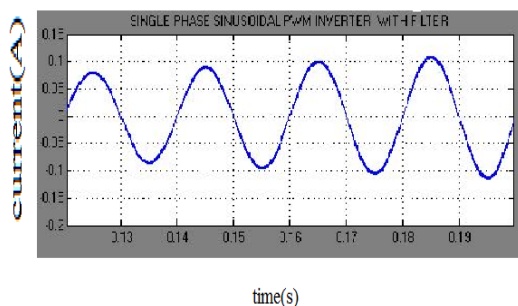


Fig 8 . Inverter Output current waveform

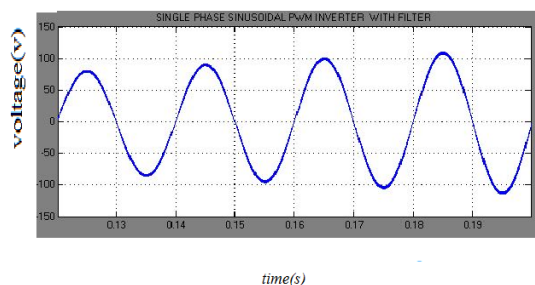


Fig 9 .Inverter Output voltage waveform

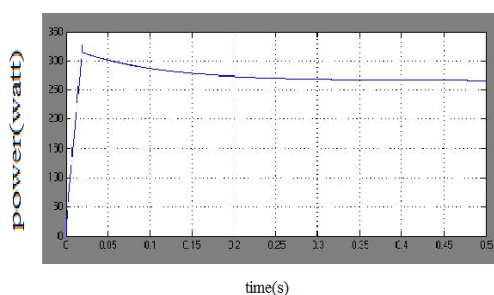


Fig10 .Solar panel output power waveform

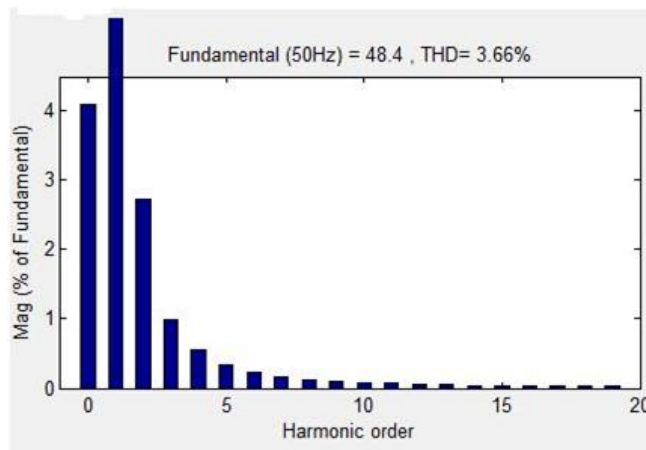


Fig 11. Proposed inverter Closed loop THD value

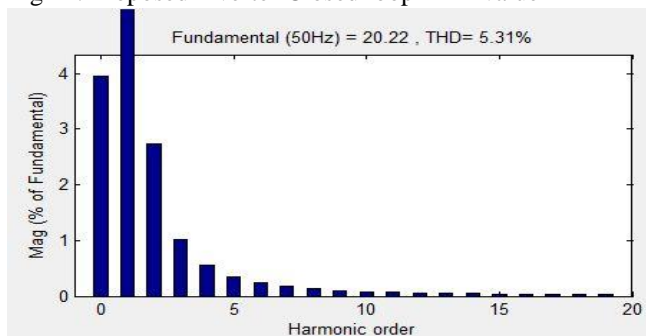


Fig 12 .Proposed inverter open loop THD value

V. CONCLUSION

In this paper, using bidirectional switches, for various stage flyback inverter was introduced for grid-connected microinverters. The soft-switching of the primary MOSFET was made possible by allowing a current flow from the grid side to the transformer. This concept was implemented by replacing the power MOSFET and the diode on the secondary side of conventional flyback inverter with bidirectional switches. Based on the modeling, a PI control scheme was implemented for control of both open loop and close loop compare THD value.

REFERENCES

- [1] N. Kasa, T. Iida, and L. Chen, "Flyback inverter controlled by sensorless current MPPT for photovoltaic power system," IEEE Trans. Ind. Electronics, 2005, vol. 52, no. 4, pp. 1145–1152.
- [2] A. C. Kyritsis, E. C. Tatakis, "Optimum design of the current-source flyback inverter for decentralized grid-connected photovoltaic systems," IEEE Trans. Energy Convers., 2008, vol. 23, no. 1, pp. 281–293.
- [3] Y. Li and R. Oruganti, "A flyback-CCM inverter scheme for photovoltaic AC module application," in Proc. AUPEC, 2008, pp. 1–6.
- [4] Y.-H. Kim, J.-G. Kim, Y.-H. Ji, C.-Y. Won, and T.-W. Lee, "A new control strategy of active clamped flyback inverter for a photovoltaic AC module system" in Proc. IEEE 8th ICPE/ECCE, 2011, pp. 1–5.
- [5] F. Tian, F. Chen, K. Rustom, and I. Batarseh, "Pulse frequency modulation with soft-switching flyback single-stage inverter," in Proc. 32nd INTELEC, 2010, pp. 1–6.
- [6] Y.-H. Ji, D.-Y. Jung, J.-H. Kim, C.-Y. Won, and D.-S. Oh, "Dual mode switching strategy of flyback inverter for photovoltaic AC modules," in Proc. IPEC, 2010, pp. 2924–2929.

- [7] V. Vorperian, "Simplified analysis of PWM converters using model of PWM switch. Continuous conduction mode," IEEE Trans. Aerospace. Electron. Syst., vol. 26, no. 3, 1990, pp. 490–496.
- [8] V. Vorperian, "Simplified analysis of PWM converters using model of PWM switch. II. Discontinuous conduction mode," IEEE Trans. Aerospace. Electron. Syst., 1990, vol. 26, no. 3, pp. 497–505.
- [9] J. Lempinen and T. Suntio, "Modeling and analysis of a self-oscillating peak-current controlled flyback converter," in Proc. 27th Annu. Conf. IEEE IECON, 2001, vol. 2, pp. 960–965.
- [10] J. Chen, R. Erickson, and D. Maksimovic, "Averaged switch modeling of boundary conduction mode DC-to-DC converters," in Proc. 27th Annu. Conf. IEEE IECON, 2001, vol. 2, pp. 844–849.
- [11] T. Suntio, "Average and small-signal modeling of self-oscillating flyback converter with applied switching delay," IEEE Trans. Power Electron., 2006, vol. 21, no. 2, pp. 479–486.
- [12] D. M. Robert and W. Erickson, "Fundamentals of Power Electronics". Norwell, MA, USA: Kluwer, 2001.
- [13] N. Tang, (2009) "Designing ultrafast loop response with type III compensation for current mode step-down converters," Texas Instruments, Dallas, TX, USA, Appl. Rep. - SLVA352A, 2009.
- [14] Application Note V1.1 D. D. Graovac, M. Purschel, and A. Kiep, "MOSFET Power Losses Calculation from Datasheet parameters, 2006, Application Note V1.1.
- [15] S. B. Kjaer, J. K. Pedersen, and F. Blaabjerg, "A review of single-phase grid-connected inverters for photovoltaic modules," IEEE Trans. Ind. Appl., 2005, vol. 41, no. 5, pp. 1292–1306.
- [16] M. Calais, J. Myrzik, T. Spooner, and V. G. Agelidis, (2002) "Inverters for single phase grid connected photovoltaic systems—An overview," in Proc. IEEE 33rd Ann. PESC, 2002, pp. 1995–2000.
- [17] Q. Li and P. Wolfs, "A review of the single phase photovoltaic module integrated converter topologies with three different DC link configurations" IEEE Trans. Power Electronics, 2008, vol. 23, no. 3, pp. 1320–1333.
- [18] Q. Mo, M. Chen, Z. Zhang, M. Gao, and Z. Qian, "Research on a non-complementary active clamp flyback converter with unfolding DC-AC inverter for decentralized grid-connected PV systems," in Proc. IEEE ECCE, 2011, pp. 2481–2487.